Electro-precipitation of magnetite nanoparticles: An electrochemical study

Mona Ibrahim [a], Karine Groenen Serrano [b,*,1], Laure Noe [a], Cécile Garcia [a], Marc Verelst [a]

[a] Centre d'Elaboration de Matériaux et d'Etudes Structurales, UPR N° 8011 – Université Toulouse III, B.P. 94347, 29 rue Jeanne Marvig, 31055 Toulouse Cedex, France
[b] Laboratoire de Génie Chimique, CNRS, Université Paul Sabatier, 118 route de Narbonne, 31062 Toulouse Cedex, France

A B S T R A C T

Nanoparticles of magnetites (Fe_3O_4) are synthesized with a new process based on electro-precipitation in ethanol medium. A mechanism pathway is proposed consisting of a $Fe(OH)_3$ precipitation followed by the reduction of iron hydroxide to magnetite in the presence of hydroxyl ions which are generated at the cathode.

1. Introduction

The prospect of a new generation of materials and devices based on nanoparticles (NPs) is a major driving force in the rapidly emerging field of nanoscale research. Magnetic NPs, and more particularly magnetite (Fe_3O_4) and maghemite (γFe_2O_3), have been widely used for biomedical applications such as cell targeting, cell separation, drug delivery, hyperthermia [1–5], or in environmental sciences, for metal separation from wastewater [6,7]. Due to their magnetic moment, magnetic NPs can be driven by an applied magnetic field into specific regions of the human body for *in vivo* applications. For *in vitro* diagnosis or for metal separation, magnetic separation and selection can be done. For these applications, magnetic NPs have to become magnetized at low magnetic field. However, in order to avoid any agglomeration phenomenon, the magnetic NPs must not present magnetic remanence, i.e. must have a zero magnetization in the absence of an applied magnetic field. This particular behavior is achieved with superparamagnetic NPs. Typically, magnetite nanoparticles become superparamagnetic at sizes below 15 nm [8].

Chemical synthesis of colloidal magnetite has been known for a long time: aqueous mixture of ferric and ferrous salts are mixed with an alkali in order to induce the precipitation of magnetite particles (maghemite can then be obtained by soft oxidation of magnetite) [9]. The average diameter of particles can be tuned between 5 and 100 nm by varying experimental conditions (concentration, temperature, nature of alkali, ionic strength, agitation. . .) but the system is always polydispersed in size [9–11] due to the Oswald ripening mechanism (the large particles will grow at the cost of the small ones) [12]. Organized assemblies or complex structures have been used as nanoreactors (microemulsion, vesicle, polymer matrix media synthesis) in order to obtain nearly monodispersed ultrafine iron oxide NPs. Some interesting reviews summarize all these techniques [13,14].

In practice, even if better control can actually be done over the size and the size distribution of NPs, progress in the use of superparamagnetic NPs depends on the improvement of synthetic methods. Though electrocoagulation in aqueous media of magnetite has been first reported in 2001 by Tsouris and colleagues [15,16], then by other researchers [17,18], these first studies reported only on supramicronic aggregates [15–17] or thin film [18] elaboration. It was only very recently (2008) that new processes were carried out, based on electro-precipitation of magnetite [19] or maghemite [20] in aqueous media, that yields nanoparticles with a controlled size distribution. In this study [19], the process allows to elaborate particles in the range size of 20–30 nm in the presence of surfactant. At the same time, we presented [21] a new process consisting of a cathodic electro-precipitation in an ethanol–water media, that yields very fine nanoparticles with a controlled size distribution (4–9 nm; std#15%) without the use of surfactant. This first paper concerned the first results with empirical data showing the influence of experimental conditions, particularly current density on the size distribution of the magnetite particles.

The aim of this article is to report an electrochemical study in order to propose a mechanism pathway for the elaboration of magnetite by electro-precipitation.

* Corresponding author. Tel.: +33 561558677; fax: +33 561556139.
E-mail address: serrano@chimie.ups-tlse.fr (K.G. Serrano).
[1] ISE member.

2. Experimental

Cyclic voltammograms were carried out in a conventional three-electrode cell using a computer controlled Voltalab potentiostat PGZ 100 model. A vitreous carbon disk (0.07 cm^2) was used as working electrode, an Ag/AgCl/Cl^-(1 M) as a reference separated with an agar–agar junction and a platinum rod as counter electrode.

Electrolysis were performed in a cell containing 90 cm^3 of $Fe(NO_3)_3{\cdot}9H_2O$ solutions in ethanol (absolute commercial 99.5% ethanol, water = 0.5% max) in the concentration range (0.01–0.16 M). During the experiment, the solution was stirred using a magnetic bar. The anode and cathode were graphite rods (0.5 cm diameter) with a geometric area of 4.7 cm^2. Electrical current was provided by an ISO-Tech Laboratory DC Power Supply model IPS-1630D. The range of potential between the anode and the cathode to produce Fe_3O_4 nanoparticles is 20–60 V. Magnetite particles were collected on the cathode as black magnetic macroscopic platelets and washed with ethanol before being dried under air at room temperature.

Iron (III) concentration evolution in the electrolyte during the electro-precipitation process is followed using a UV–visible–NIR spectrometer (Varian cary 5000) using the Beer–Lambert's law (λ_{abs} = 340 nm).

3. Results and discussion

Typical Fe_3O_4 nanoparticles elaborated by the electro-precipitation procedure are shown in Fig. 1. As shown on the picture, those particles have an average mean size centered on 6.2 nm with a quite narrow distribution (standard deviation = 18%). Because the nanoparticles produced are free of any surfactant, they show a strong tendency to be agglomerated and form a solid powder. However, after the electrosynthesis, one can disperse them in a given matrix by choosing the appropriate surfactant. Producing nanoparticles free of any surfactant is a true advantage, ensuring interesting handling possibilities. The characterization of these particles was reported in a previous paper [21].

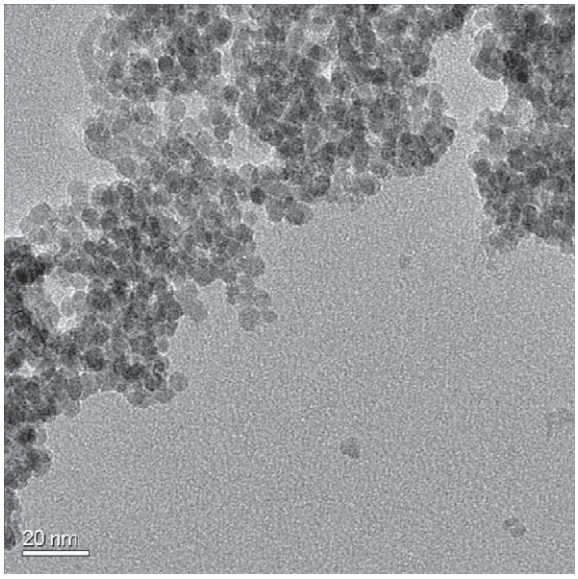

Fig. 1. Transmission electron microscopy photograph for typical Fe_3O_4 nanoparticles. Experimental conditions: $Fe(NO_3)_3{\cdot}9H_2O = 2 \times 10^{-2}$ M in ethanol, 30 mA cm^{-2}. Size: Φ = 6.2 nm (std = 18%).

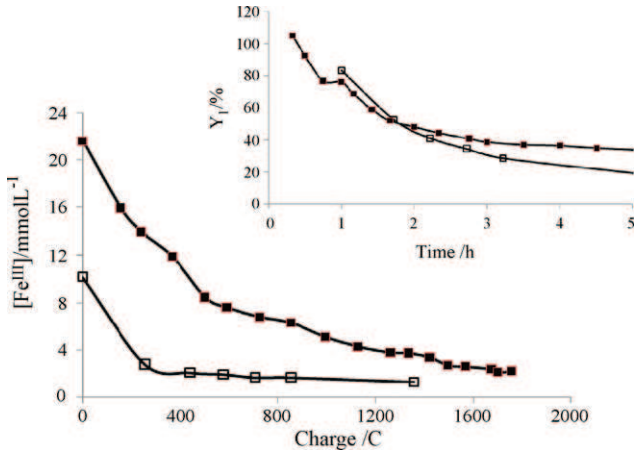

Fig. 2. Variation of the Fe^{3+} concentration and the current efficiency Y (Eq. (2)) (inset panel) with charge during the electro-precitation process. (■) $[Fe^{III}] = 2 \times 10^{-2}$ M, i = 30 mA cm^{-2} and (□) $[Fe^{III}] = 10^{-2}$ M, i = 15 mA cm^{-2} in ethanol.

3.1. On the Fe^{3+} reduction

Fig. 2 shows the evolution of Fe^{3+}concentration versus the electrical charge and the variation of the instantaneous current efficiency Y_1 corresponding to the Fe^{3+} disappearance with time (inset panel) during the electrochemical process for two initial concentrations of iron nitrate (10^{-2} and 2×10^{-2} M). Y_1 is calculated considering the global reaction (1) which will be discussed at the end of the paper:

$$3Fe^{3+} + 2NO_3{}^- + 2H_2O + 9e^- \rightarrow Fe_3O_4 + 2NO_2{}^- + 2H_2 \quad (1)$$

Elaboration of one mole of magnetite needs three moles of Fe^{3+} ions and nine moles of electrons. Consequently the instantaneous current efficiency Y_1, can be expressed by the relation (2):

$$Y_1(\%) = \frac{(n^{\circ}_{Fe^{3+}} - n_{Fe^{3+}})9F}{3It}100 \quad (2)$$

where $n^{\circ}_{Fe^{3+}}$ and $n_{Fe^{3+}}$ are respectively the number of Fe^{III} moles at initial time and at time t (s). Fig. 2 shows clearly, for both initial concentrations (10^{-2} and 2×10^{-2} M), that the current efficiency Y_1 is higher than 80% at the beginning of the process. However, it decreases quickly during the electrolysis. Note that a low Y_1 is not directly correlated to a weak Fe^{3+}concentration. Indeed, even for the lowest initial concentration experiment (10^{-2} M), the Y_1 values versus time are very close for both concentrations. The efficiency decreases continuously even if addition of iron nitrate in ethanol is carried out during the process. These results seem to show that an inhibition phenomenon has occurred on the cathode. This inhibition results probably from the very low electrical conductivity of magnetite deposited on the cathode, since, the ratio of electrical conductivity between graphite and magnetite is higher than 10^5 [22–24].

3.2. On the magnetite production

In order to study the influence of the concentration of the precursor Fe^{III} on the magnetite production, series of galvanostatic electrolysis were carried out at different concentrations. Up to 4×10^{-2} M, a pure black magnetite is obtained. However, beyond this value, the collected product is polluted by brownish pollution. Beyond 8×10^{-2} M only a non-magnetic amorphous precipitate is collected (iron III hydroxide [21]). This behavior is explained by the excess of water molecules at high nitrate concentration which causes the iron hydroxide production. An electrolysis was carried out with $FeCl_3$ (anhydrous) as iron precur-

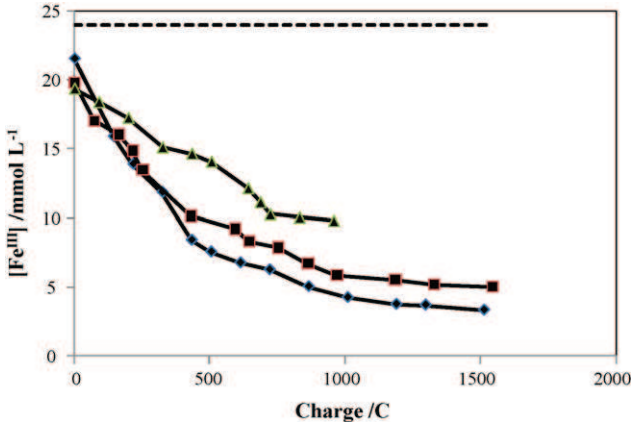

Fig. 3. Variation of the Fe^{3+} concentration with charge during the electro-precitation process for three current densities ((---) 2.3 mA cm^{-2}, (▲) 6.4 mA cm^{-2}, (■) 12.7 mA cm^{-2}, (♦) 25.5 mA cm^{-2}), $[Fe(NO_3)_3{\cdot}9H_2O] = 2 \times 10^{-2}$ M in ethanol.

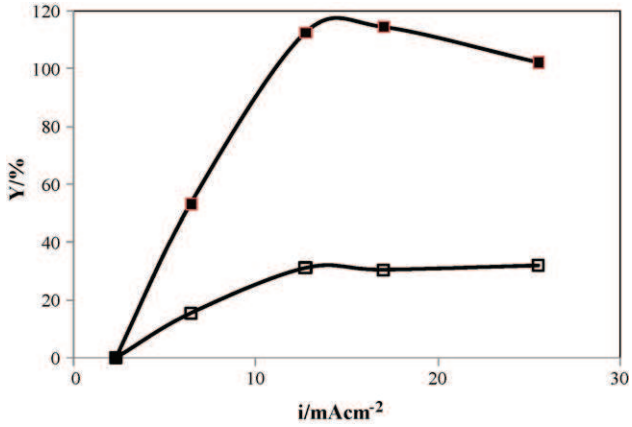

Fig. 4. Variation of Y_2: (■) (corresponding to Eq. (3)) and Y_3: (□) (corresponding to Eq. (4)): with current densities after 1200 As of electrolysis $[Fe(NO_3)_3{\cdot}9H_2O] = 2 \times 10^{-2}$ M in ethanol.

sor instead of $Fe(NO_3)_3{\cdot}9H_2O$. No particles were produced and the Fe^{3+} concentration fluctuated slightly around the initial concentration (2×10^{-2} M ± 0.02) and remained almost constant even after a long electrolysis time (not shown). Fe^{3+} ions are reduced into Fe^{2+} at the cathode but those ferrous ions migrate to the anode to be oxidized into Fe^{3+} again. We conclude that nitrate and also little water must be present to produce Fe_3O_4 particles on the cathode.

Preliminary results reported elsewhere [21] have shown that current density is an important parameter. Fig. 3 reports the evolution of Fe^{3+} concentration with the charge at four current densities (2.3, 6.4, 12.7, 25.5 mA cm^{-2}) during electrolyses performed at initial Fe^{3+} concentration equal to 2×10^{-2} M. Fig. 3 highlights that the Fe^{3+} reduction/precipitation phenomenon is more efficient using high current density. Moreover at the lowest current density, the Fe^{3+} concentration is constant, there is no formation of magnetite.

After each electrolysis, corresponding to 1200 As, the particles were collected, dried and weighted, the efficiency of the process is evaluated following two equations:

- On one hand, by comparison of the quantity of Fe_3O_4 particles produced with the number of Fe^{3+} ions disappearing into the bath considering Eq. (1):

$$Y_2(\%) = \frac{3n_{Fe_3O_4}}{(n^{\circ}_{Fe^{3+}} - n_{Fe^{3+}})} 100 \quad (3)$$

- On the other hand, the evolution of the faradic efficiency for magnetite production is calculated following Eq. (4):

$$Y_3(\%) = \frac{9Fn_{Fe_3O_4}}{IT} 100 \quad (4)$$

For current densities higher than, or equal to 13 mA cm^{-2}, 100% of Fe^{3+} ions reduced at the cathode are used to produce magnetite but it collapses dramatically (52%) for 6.4 mA cm^{-2} and becomes 0% at 2.3 mA cm^{-2} confirming that magnetic production needs a minimum current density. One can note that $Y_2 > 100\%$ is due to mass incertitude: Fe_3O_4 nanopowders were not dried at high temperature to avoid Fe_2O_3 formation. The maximum current efficiency for magnetite production is close to 30%. This weak value can be explained by the inactivation of the cathode resulting from the formation of magnetite particles during the process.

3.3. Cyclic voltamperometric study

Fig. 4 shows cyclic voltamogramms of $Fe(NO_3)_3{\cdot}9H_2O$ (10^{-2} mol L^{-1}) in pure ethanol. Four reduction peaks appear during the reduction process at respectively 0.5, 0.07, −1.15 and −2.35 V/ref. (see peaks I–IV, Fig. 5). The anodic peaks I′ and III′ are associated with peaks I and III respectively. To identify the reduction processes which occur at these potentials, addition of $LiNO_3$, $FeCl_3$ salts and water were carried out. The inset panels in Fig. 5 present the intensity of peaks variation with addition of compounds.

The addition of $FeCl_3$ anhydrous salts provokes a proportional increasing of the peak I intensity. Thus, peak I corresponds to the reduction of iron III ($Fe^{III} + e^- \rightarrow Fe^{II}$). Similarly, the reduction peak IV varies proportionally with the concentration of nitrate ions. Thus we conclude that nitrate reduction occurs at very low potential ($NO_3^- + H_2O + 2e^- \rightarrow NO_2^- + 2OH^-$). Nitrite generation has been detected during electrolysis of $Fe(NO_3)_3{\cdot}9H_2O$ solutions in previous study [21].

The intensity of peak III increases proportionally with addition of water, peaks I and IV are not affected. These peaks are directly correlated to water reduction:

$$H_2O + e^- \rightarrow (1/2)H_2 + OH^-$$

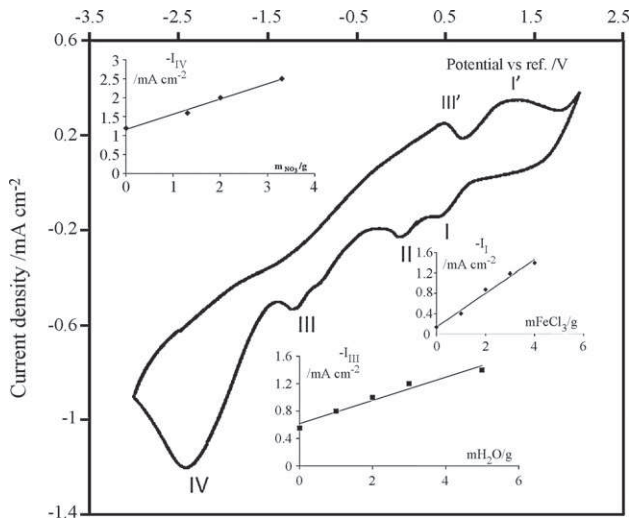

Fig. 5. Cyclic voltamogramm obtained in ethanol containing $[Fe(NO_3)_3{\cdot}9H_2O] = 2 \times 10^{-2}$ M. Working electrode: graphite, auxiliary electrode: Pt, Ref. electrode: Ag/AgCl/Cl$^-$. Scan rate: 100 mV/s with addition of water or $FeCl_3$ or nitrate ions.

Peak II (0.07 V/ref.) which decreases under argon atmosphere seems to correspond to the reduction of dissolved oxygen ($(1/2)O_2 + 2H^+ + 2e^- \rightarrow H_2O$) in water.

4. Conclusions

After this work we can summarize main results and we can establish some rules to electro-precipitate Fe_3O_4 NPs in ethanol bath:

- A Fe^{3+} source is necessary. Fe^{3+} ions are reduced at the cathode into Fe^{2+} at a potential between 0 and 1 V/ref.
- These Fe^{2+} ions precipitate at the cathode under Fe_3O_4 NPs only if the ethanolic bath contains water and nitrates. However, too much water leads to hydroxide production and not magnetite NPs.
- Reduction waves of water and nitrates occur at much more negative potential than iron reduction and produce OH^- ions.
- Only high current density produces Fe_3O_4 NPs corresponding to a maximum faradic efficiency (Y_3) equals to 30%. The cyclic voltamogramm evidences that at low current density, reduction waves of water and nitrates are not reached. Fe^{3+} ions are well reduced into Fe^{2+}, but the local pH at the cathode vicinity is not basic enough to precipitate Fe_3O_4 NPs. Consequently, Fe^{2+} migrates to the anode to be reoxidized.
- In a solution including Fe^{3+} and nitrate ions, traces of water and using high current density, 100% of the current is used for Fe^{3+} reduction at the beginning of the electro-precipitation process but decreases gradually during the process as Fe_3O_4 NPs are formed whatever the inital concentration of Fe^{III}. Probably Fe_3O_4 NPs are inhibited further by a passivation electrode phenomenon.

  The experimental results allowed us to propose the following reactional mechanism for Fe_3O_4 NPs electro-precipitation in an ethanolic/water bath (Eqs. (5)–(7)).
- OH^- ions are generated at the cathode during the water and nitrates reduction:

$$NO_3^- + H_2O + 2\bar{e} \rightarrow NO_2^- + 2OH^- \quad (5)$$

$$2H_2O + 2\bar{e} \rightarrow H_2 + 2OH^- \quad (6)$$

- The pH increase at the vicinity of cathode causes $Fe(OH)_3$ precipitation.
- Then, the iron (III) hydroxide is reduced to magnetite (Fe_3O_4) following the reaction:

$$3Fe(OH)_3 + e^- \rightarrow Fe_3O_4 + 4H_2O + OH^- \quad (7)$$

Note that this last reaction regenerates the water consumed in nitrate and water reduction. Remark also, that this last reaction is an equilibrium. Consequently in presence of an excess of water in the solution, Fe_3O_4 NPs are not formed and $Fe(OH)_3$ remains stable.

Finally, the process can be written more globally following this last equation:

$$3Fe^{3+} + 2NO_3^- + 2H_2O + 9e^- \rightarrow Fe_3O_4 + 2NO_2^- + 2H_2$$

References

[1] K. Dormer, C. Seeney, K. Lewelling, G. Lian, D. Gibson, M. Johnson, Biomaterials 26 (2005) 2061.
[2] P. Tartaj, M. del Puerto Morales, S. Veintemillas-Verdaguer, T. González-Carreño, C.J. Serna, J. Phys. D: Appl. Phys. 36 (2003) R182.
[3] D.H. Kim, K.N. Kim, K.M. Kim, Y.K. Lee, J. Biomed. Mater. Res. Part A 88 (2009) 1.
[4] A. Aqil, S. Vasseur, E. Duguet, C. Passirani, J.P. Benoît, A. Roch, R. Müller, R. Jérôme, C. Jérôme, J. Magn. Magn. Mater. 321 (2008) 373.
[5] T. Murakami, K. Tsuchida, Mini-Rev. Med. Chem. 8 (2008) 174.
[6] A.-F. Ngomsik, A. Bee, M. Draye, G. Cote, V. Cabuil, C.R. Chim. 8 (2005) 963.
[7] C.J.M. Chin, P.W. Chen, L.J. Wang, Chemosphere 63 (2006) 1809.
[8] S. Bedanta, W. Kleemann, J. Phys. D: Appl. Phys. 42 (2009); J. Appl. Phys. 105 (2009) 07C306, doi:10.1063/1.3070645.
[9] R. Massart, IEEE Trans. Magn. Mater. 17 (1981) 131.
[10] R. Massart, V. Cabuil, J. Chem. Phys. 84 (1987) 967.
[11] A. Bee, R. Massart, S. Neveu, J. Magn. Magn. Mater. 6 (1995) 149.
[12] R. Boistelle, J.P. Astier, J. Cryst. Growth 90 (1988) 14.
[13] A.-K. Gupta, M. Gupta, Biomaterials 26 (2005) 3995.
[14] U. Jeong, X.W. Teng, Y. Wang, H. Yang, Y.N. Xia, Adv. Mater. 19 (2007) 33.
[15] C. Tsouris, D.W. Depaoli, J.T. Shor, M.Z.C. Hu, T.Y. Ying, Colloids Surf. A 111 (2001) 223.
[16] T.Y. Ying, S. Yiacoumi, C. Tsouris, J. Disper. Sci. Technol. 23 (2002) 569.
[17] S. Franger, P. Berthet, J. Berthon, J. Solid State Electrochem. 8 (2004) 218.
[18] L. Martinez, D. Leinen, F. Martin, J. Electrochem. Soc. 154 (2007) D126.
[19] L. Cabrera, S. Gutierrez, N. Menendez, M.P. Morales, P. Herrasti, Electrochem. Acta 53 (2008) 3436.
[20] H. Park, P. Ayala, M.A. Deshusses, A. Mulchandani, H. Choi, N.V. Myung, Chem. Eng. J. 139 (2008) 208.
[21] R.F.C. Marques, C. Garcia, P. Lecante, S.J.L. Ribeiro, L. Noé, N.J.O. Silva, V.S. Amaral, A. Millan, M. Verelst, J. Magn. Magn. Mater. 320 (2008) 2311.
[22] S. Dutta, S.K. Manik, M. Pal, S.K. Pradhan, P. Brahma, D. Chakravorty, J. Magn. Magn. Mater. 288 (2005) 301.
[23] E. Wilson, E.F. Herroun, Proc. R. Soc. Lond. A 105 (1924) 334–345.
[24] R.L. Powell, G.E. Childs, American Institute of Physics Handbook, vol. 4, 1972, p. 142.